Optical Soliton Dynamics in Nonlinear Evolution Equations: Modified Kawahara and Modified Benjamin Bona Mahony Models

Hadia Khalid Mehmood[1], Dumitru Baleanu[2], Muhammad Abbas[1], Majeed Ahmad Yousif[3,*], Pshtiwan Othman Mohammed[4,5,*], Farah Aini Abdullah[6] and Ibrahim Sulaiman Ibrahim[3]

[1] Department of Mathematics, University of Sargodha, Sargodha, 40100, Pakistan

[2] Department of Computer Science and Mathematics, Lebanese American University, Beirut, 11022801, Lebanon

[3] Department of Mathematics, College of Education, University of Zakho, Zakho, 42002, Iraq

[4] Department of Mathematics, College of Education, University of Sulaimani, Sulaymaniyah, 46001, Iraq

[5] International Telematic University Uninettuno, Corso Vittorio Emanuele II, 39, Roma, 00186, Italy

[6] School of Mathematical Sciences, Universiti Sains Malaysia, Penang, 11800, Malaysia

INFORMATION

Keywords:
Modified Kawahara (mK) equation
modified Benjamin Bona Mahony (mBBM) equation
Optical Soliton Solutions

MSC:
35C08
35C09
35Q51

DOI: 10.23967/j.rimni.2025.10.67550

Revista Internacional de Métodos Numéricos para Cálculo y Diseño en Ingeniería

Optical Soliton Dynamics in Nonlinear Evolution Equations: Modified Kawahara and Modified Benjamin Bona Mahony Models

Hadia Khalid Mehmood[1], Dumitru Baleanu[2], Muhammad Abbas[1], Majeed Ahmad Yousif[3,*], Pshtiwan Othman Mohammed[4,5,*], Farah Aini Abdullah[6] and Ibrahim Sulaiman Ibrahim[3]

[1]Department of Mathematics, University of Sargodha, Sargodha, 40100, Pakistan

[2]Department of Computer Science and Mathematics, Lebanese American University, Beirut, 11022801, Lebanon

[3]Department of Mathematics, College of Education, University of Zakho, Zakho, 42002, Iraq

[4]Department of Mathematics, College of Education, University of Sulaimani, Sulaymaniyah, 46001, Iraq

[5]International Telematic University Uninettuno, Corso Vittorio Emanuele II, 39, Roma, 00186, Italy

[6]School of Mathematical Sciences, Universiti Sains Malaysia, Penang, 11800, Malaysia

ABSTRACT

This paper explores the dynamic behavior of optical soliton solutions for the modified Kawahara (mK) equation and the modified Benjamin-Bona-Mahony (mBBM) equation, two significant nonlinear evolution equations. Using an advanced analytical approach, a diverse set of soliton solutions is derived, including bell-shaped, anti-bell-shaped, W-shaped, M-shaped, and periodic waveforms. These solutions unveil the intricate nonlinear dynamics underlying the equations. The robustness of the method is demonstrated through comprehensive 2D, 3D, and contour visualizations, offering clear insights into the physical significance of the solitons. The study enhances the existing catalog of soliton solutions, contributing to a deeper understanding of nonlinear wave propagation and its potential applications in fields such as optical communication and fluid dynamics.

OPEN ACCESS

Received: 06/05/2025

Accepted: 09/06/2025

Published: 15/08/2025

DOI
10.23967/j.rimni.2025.10.67550

Keywords:
Modified Kawahara (mK) equation
modified Benjamin Bona Mahony (mBBM) equation
Optical Soliton Solutions

MSC: 35C08; 35C09; 35Q51

1 Introduction

Nonlinear equations involve variables interacting in non-proportional ways, often through powers or products. These equations, common in fields like physics and biology, model complex phenomena such as chaos and solitons, producing intricate and diverse solutions [1,2]. Optical solitons are particularly notable for their ability to propagate through a medium while maintaining a stable, localized form in nonlinear optics [3]. This stability arises from the medium's nonlinear refractive index, which counteracts dispersion, allowing the soliton to maintain its shape during propagation

*Correspondence: Majeed Ahmad Yousif, Pshtiwan Othman Mohammed (majeed.yousif@uoz.edu.krd, pshtiwansangawi@gmail.com).

[4,5]. The study of such nonlinear dynamics extends beyond optics to include space mission design, where nonlinear equations govern trajectory transfers influenced by perturbations, as seen in Earth–Moon libration point studies [6]. Due to the complexity of nonlinear variables, obtaining analytical solutions can be challenging [7], prompting scientists to rely on computational methods as essential tools for analysis and problem-solving [8]. Numerical methods and algorithms have been widely employed in the study of nonlinear evolution equations (NLEEs) to facilitate effective investigation using advanced technical tools [9]. These approaches have been developed to explore nonlinear systems, offering scholars valuable insights into their properties [10].

Soliton solutions play a vital role in understanding nonlinear Partial Differential Equations (PDEs) due to their stability and localization properties. Various forms have been explored, including hyperbolic-sine-Gaussian [11] and complex-valued hyperbolic-cosine-Gaussian solitons [12], highlighting structured light propagation in nonlinear media. Boomerons in coupled NLS systems [13] and butterfly-shaped nonautonomous solitons [14] illustrate dynamic behaviors influenced by dispersion and external controls. Exact soliton solutions have also been found under anti-cubic [15] and quartic Rosenau-Kawahara-type nonlinearities [16]. Recent work extends this analysis to solitons governed by fractional derivatives in the CGL equation [17] and high-dimensional models like the (2+1)-dimensional Jaulent-Miodek equation [18], showing the broad applicability of soliton theory in complex physical systems.

Researchers use mathematical techniques to analyze the stability, solution structures, and dynamic behaviors of these equations, aiming to understand fundamental physical phenomena [19]. Among various NLEEs, the modified Kawahara equation has attracted significant attention from researchers [20]. Its analytical solutions find applications in technical and mechanical fields such as fluid dynamics, plasma physics, and nonlinear optics [21]. The study of wave phenomena in diverse physical systems is essential for understanding dispersive and nonlinear effects, making the mK equation a valuable tool for exploring nonlinear wave propagation [22–24]. Its unique properties have generated widespread interest [25], particularly the soliton-like solutions that preserve their characteristics during propagation, crucial for understanding nonlinear wave phenomena [26]. Solitary wave solutions are vital for interpreting complex waveforms and motion [27]. Additionally, the mK equation is employed to investigate wave interactions involving both dispersive and nonlinear effects, contributing to the study of wave dynamics and complex behaviors [28]. Finally, the mK equation has significant implications across various scientific and engineering fields, underscoring its importance in the study of nonlinear optics, plasma waves, and water waves [29]. The mK equation can be defined numerically as [30–33]:

$$\Psi_t + \Psi^2 \Psi_r + \kappa \Psi_{rrr} + \varkappa \Psi_{rrrrr} = 0, \tag{1}$$

where $\Psi = \Psi(r,t)$ indicates an optical wave's complex electric field amplitude as a consequence of its location r along with the time t. The parameter κ specifies the extent of the third-order dispersion factor, affecting dispersion in geographical areas where waves with various frequencies flow at different velocity levels [34]. The greater level of κ enhances the dispersive result, which modifies the wave's form and characteristics of propagation [35]. Furthermore, $\varkappa$ modulates the elevation of the fifth-order dispersion form, adjusting dispersive impacts on a higher order. Similar to κ, $\varkappa$ affects the wave's stability form and interaction behavior, implementing difficulties concerning the propagation of waves [36]. Eq. (1) is significant in nonlinear wave science as it models the interplay between nonlinearity and higher-order dispersion, enabling the description of stable nonlinear waves such as solitons. This balance is crucial for understanding wave propagation, stability, and interactions in various physical and engineering contexts.

The equation $\Phi_t + \Phi_r + \Phi^n\Phi_r + \theta\Phi_{rrt=0}$, known as BBM, is the most well-known framework for practical production. Long waves in a nonlinear dispersive system have been represented by this equation. There is evident soliton-like behavior in the outcome of the BBM equation, which is unable to be explained by any existing theory [37]. The study of surface waves in liquids, acoustic-gravity waves in compressible fluids, hydromagnetic waves in cold plasma, and acoustic waves in harmonic crystals are among the uses of the BBM equation. For $n = 2$, the BBM equation is known as the mBBM [38]. The soliton-like behavior of the mBBM equation conflicts with established hypotheses. This paper analyzes the exact traveling wave solutions of the mBBM problem utilizing the Ansatze strategy [39]:

$$\Phi_t + \Phi_r + \Phi^2\Phi_r + \theta\Phi_{rrt=0}, \tag{2}$$

where $\Phi(r, t)$ is an undefined function in terms of the positional variable r and the time dimension t, where θ represents insufficient constants. Khan and Akbar [40] utilized the $(-\phi(\xi))$ expansion method for the exact solitary wave solutions to the mBBM problem. These solutions include solutions through hyperbolic functions, trigonometric functions, and rational functions. Khan et al. [41] have established traveling wave solutions for the mBBM problem by using the modified simple equation methodology. The solitonary periodic and exact traveling wave solutions of this equation have been examined with a number of efficient techniques, such as the homogeneous balance method by Rady et al. [42], an algebraic method by Tang et al. [43], the variable-coefficient balancing-act method by Chen et al. [44], and the Jacobi elliptic function expansion method by An and Zhang [45], the factorization technique by Estévez et al. [46]. Using a modification, Mammeri [47] discovered some long time limitations for the periodic BBM equation. The generalized BBM and Burgers-BBM equations feature some novel periodic and soliton solutions that have been found by Gomez et al. [48] using the tanh–coth approach. Gomez and Salas [49] have recently combined the variational iteration approach and the exp-function method to create traveling wave solutions for this problem. In this paper, we employ the Sardar sub-equation approach [50–53] to derive a range of novel optical soliton solutions for the mK equation and the mBBM equation. By applying this innovative method, we obtain several new soliton solutions that have not been reported previously in the literature. Additionally, we identify the specific criteria that must be met for these solutions, offering a comprehensive analysis of their properties and implications. The choice of the mmK and the mBBM equations is motivated by their significance in describing nonlinear wave phenomena in dispersive media, such as optical fibers and shallow water surfaces. These models account for higher-order dispersion and nonlinear effects, making them ideal for investigating complex soliton dynamics. The application of the Sardar sub-equation method to these equations offers a direct and effective way to derive diverse soliton structures, highlighting the method's strength in capturing rich nonlinear behaviors not previously reported in the literature. Moreover, this method provides advantages such as reduced computational complexity, the ability to handle a wide range of nonlinearities, and the generation of more general exact solutions compared to traditional analytical techniques. The following summarizes the paper's thorough and extensive structure: We go into further detail about the SSE method for figuring out the exact solution of NLEEs in Section 2. The method are utilized to obtain the precise solution for the mK equation and mBBM equation in Section 3. Graphical illustrations and physical meaning of the graphs are presented in Section 4 and Section 5. At last, conclusion is provided in Section 6.

2 Description of Sardar Sub-Equation Method

This section explains the SSE method, used to determine traveling wave solutions of NLEEs. The method simplifies the equations, allowing for the extraction of exact soliton solutions that reveal the underlying dynamics of the system." In this study, we progress by following the below key steps:

- **Step 1:**

$$F(\phi, \phi_r, \phi_t, \phi_{rr}, \phi_{tt}, ...) = 0, \tag{3}$$

where F represents the polynomial of $\Psi(r,t)$ and $\Psi(\zeta) = \Psi(r,t)$ is the representation of the unknown function. Suppose the wave transformation

$$\zeta = r - \tau t,$$

where the orbitrary constant is denoted by τ. Eq. (3) is a general nonlinear evolution equation in terms of the unknown function $\phi(r,t)$, involving its partial derivatives. The operator F represents a nonlinear combination of ϕ and its derivatives, modeling a wide range of physical systems. This form sets the stage for reduction via the traveling wave transformation.
Taking advantage of the transformation, Eq. (3) is transformed into the subsequent Ordinary Differential Equations (ODE).

$$M(\Psi, \Psi', \Psi'', ...) = 0. \tag{4}$$

- **Step 2:** M is determined by F. In relation to ζ, prime articulate the derivaties. We regards Eq. (4) to have a formal solution.

$$\Psi(\zeta) = \sum_{s=0}^{L} v_s \Omega^s(\zeta), v_s \neq 0, \tag{5}$$

where $v_s (0 \leq s \leq L)$ are constants that will be found out later, and $\Omega(\zeta)$ fulfilling the ODE as follows:

$$\Omega'(\zeta) = \sqrt{\rho + \vartheta \Omega^2(\zeta) + \Omega^4(\zeta)}, \tag{6}$$

where ρ and ϑ are constants and Eq. (6) gives the solution as follows:
Case I: When $\vartheta > 0$ and $\rho = 0$, then

$$\Omega_1^{\pm} = \pm\sqrt{-mn\vartheta} \quad sech_{mn}\left(\sqrt{\vartheta}\zeta\right),$$

$$\Omega_2^{\pm} = \pm\sqrt{mn\vartheta} \quad csch_{mn}\left(\sqrt{\vartheta}\zeta\right),$$

where

$$sech_{mn}(\zeta) = \frac{2}{me^{\zeta} + ne^{-\zeta}}, \quad csch_{mn}(\zeta) = \frac{2}{me^{\zeta} - ne^{-\zeta}}.$$

Case II: When $\vartheta < 0$ and $\rho = 0$, then

$$\Omega_3^{\pm} = \pm\sqrt{-mn\vartheta} \quad sec_{mn}\left(\sqrt{-\vartheta}\zeta\right),$$

$$\Omega_4^{\pm} = \pm\sqrt{-mn\vartheta} \quad csc_{mn}\left(\sqrt{-\vartheta}\zeta\right),$$

where

$$sec_{mn}(\zeta) = \frac{2}{me^{\iota\zeta} + ne^{-\iota\zeta}}, csc_{mn}(\zeta) = \frac{2}{me^{\iota\zeta} - ne^{-\iota\zeta}}.$$

Case III: When $\vartheta < 0$ and $\rho = \frac{\vartheta^2}{4}$, then

$$\Omega_5^{\pm} = \pm\sqrt{\frac{-\vartheta}{2}} \quad tanh_{mn}\left(\sqrt{\frac{-\vartheta}{2}}\zeta\right),$$

$$\Omega_6^{\pm} = \pm\sqrt{\frac{-\vartheta}{2}} \quad coth_{mn}\left(\sqrt{\frac{-\vartheta}{2}}\zeta\right),$$

$$\Omega_7^{\pm} = \pm\sqrt{\frac{-\vartheta}{2}}\left(tanh_{mn}\left(\sqrt{-2\vartheta}\zeta\right) \pm \iota\sqrt{mn} \quad sech_{mn}\left(\sqrt{-2\vartheta}\zeta\right)\right),$$

$$\Omega_8^{\pm} = \pm\sqrt{\frac{-\vartheta}{2}}\left(coth_{mn}\left(\sqrt{-2\vartheta}\zeta\right) \pm \sqrt{mn} \quad csch_{mn}\left(\sqrt{-2\vartheta}\zeta\right)\right),$$

$$\Omega_9^{\pm} = \pm\sqrt{\frac{-\vartheta}{8}}\left(tanh_{mn}\left(\sqrt{\frac{-\vartheta}{8}}\zeta\right) + coth_{mn}\left(\sqrt{\frac{-\vartheta}{8}}\zeta\right)\right),$$

where

$$tanh_{mn}(\zeta) = \frac{me^{\zeta} - ne^{-\zeta}}{me^{\zeta} + ne^{-\zeta}},\ coth_{mn}(\zeta) = \frac{me^{\zeta} + ne^{-\zeta}}{me^{\zeta} - ne^{-\zeta}}.$$

Case IV: When $\vartheta > 0$ and $\rho = \frac{\vartheta^2}{4}$, then

$$\Omega_{10}^{\pm} = \pm\sqrt{\frac{\vartheta}{2}} \quad tan_{mn}\left(\sqrt{\frac{\vartheta}{2}}\zeta\right),$$

$$\Omega_{11}^{\pm} = \pm\sqrt{\frac{\vartheta}{2}} \quad cot_{mn}\left(\sqrt{\frac{\vartheta}{2}}\zeta\right),$$

$$\Omega_{12}^{\pm} = \pm\sqrt{\frac{\vartheta}{2}}\left(tan_{mn}\left(\sqrt{2\vartheta}\zeta\right) \pm \sqrt{mn} \quad sec_{mn}\left(\sqrt{2\vartheta}\zeta\right)\right),$$

$$\Omega_{13}^{\pm} = \pm\sqrt{\frac{\vartheta}{2}}\left(cot_{mn}\left(\sqrt{2\vartheta}\zeta\right) \pm \sqrt{mn} \quad csc_{mn}\left(\sqrt{2\vartheta}\zeta\right)\right),$$

$$\Omega_{14}^{\pm} = \pm\sqrt{\frac{\vartheta}{8}}\left(tan_{mn}\left(\sqrt{\frac{\vartheta}{8}}\zeta\right) \pm cot_{mn}\left(\sqrt{\frac{\vartheta}{8}}\zeta\right)\right),$$

where

$$tan_{mn}(\zeta) = -\iota\frac{me^{\zeta} - ne^{-\zeta}}{me^{\zeta} + ne^{-\zeta}},\ cot_{mn}(\zeta) = \iota\frac{me^{\zeta} + ne^{-\zeta}}{me^{\zeta} - ne^{-\zeta}}.$$

These functions, with parameters m and n, are hyperbolic and generalized trignometric functions. The trignometric and hyperbolic functions are known if we choose $m = n = 1$.

- **Step 3:** We use the numeric balances to get the integer L. We derive an algebric equation in the form of $\Omega_s(\zeta)$ by inserting Eq. (5) into Eq. (4). This equation balances by equating the powers of $\Omega^s(\zeta)$ $s = (0, 1, 2, ...)$ to zero, yielding a set of algebric equations.
- **Step 4:** The set of equations provides the travelling wave solution for the given problem as well as the parameters that are needed.

The SSE method offers a structured algebraic framework that efficiently reduces nonlinear evolution equations to solvable forms, yielding exact traveling wave solutions. Its major strengths include simplicity, flexibility in handling various parameterized forms, and the ability to produce a wide range of soliton solutions. However, the method assumes the existence of a suitable ansatz structure and relies heavily on balancing procedures, which may limit its applicability to certain classes of equations where such structures are not easily identifiable or lead to overly complex algebraic systems.

3 Execution of Sardar Sub-Equation Method

This section is divided into two parts: the first applies the SSE method to the mK equation, detailing the process of deriving traveling wave solutions and analyzing their characteristics. The second part extends the same SSE method to the mBBM equation, demonstrating its versatility and effectiveness in extracting soliton solutions for this equation as well.

3.1 Modified Kawahara Equation

In this section, we utilize the SSE method to mK equation. Employing the wave transformation $\zeta = r - \tau t$ and $\Psi(r,t) = \Psi(\zeta)$ holds Eq. (1) into ODE

$$-\tau\Psi + \Psi^2\Psi_\zeta + \kappa\Psi_{\zeta\zeta\zeta} - \varkappa\Psi_{\zeta\zeta\zeta\zeta\zeta} = 0. \tag{7}$$

Eq. (7) is derived by applying the traveling wave transformation $\zeta = r - \tau t$ to reduce the modified Kawahara equation from a PDE to an ODE. The terms represent the wave speed effect, nonlinear convection, and higher-order dispersion, which together govern the structure of traveling wave solutions.

After integrating Eq. (7) twice, we get

$$-\tau\Psi + \frac{1}{3}\Psi^3 + \kappa\Psi'' - \varkappa\Psi^{(4)} + C\Psi + D = 0, \tag{8}$$

where C and D are constants. Following the highest order derivative term $\Psi^{(4)}$ and the highest order nonlinear term Ψ^3 being balanced, $L = 2$ are achieved. Therefore, employing the SSE approach, the solution to Eq. (8) has the following form:

$$\Psi(\zeta) = v_0 + v_1\Omega(\zeta) + v_2\Omega(\zeta)^2, \tag{9}$$

where v_0, v_1, v_2 are constants. Substitute Eqs. (8), (9) into Eq. (6), using the resulting algebraic equation, we take a polynomial in the form of $\Omega^s(\zeta)$ and equal its powers to zero. We get

$$\begin{cases}
(\Omega(\zeta))^0 : D - \tau v_0 + Cv_0 + \frac{v_0^3}{3} + 2\kappa v_2\rho - 8\varkappa v_2\rho\vartheta = 0,\\
(\Omega(\zeta))^1 : -\tau v_1 + Cv_1 + v_0^2 v_1 - 12\varkappa v_1\rho + \kappa v_1\vartheta - \varkappa v_1\vartheta^2 = 0,\\
(\Omega(\zeta))^2 : v_0 v_1^2 - \tau v_2 + Cv_2 + v_0^2 v_2 - 72\varkappa v_2\rho + 4\kappa v_2\vartheta - 16\varkappa v_2\vartheta^2 = 0,\\
(\Omega(\zeta))^3 : 2\kappa v_1 + \frac{a_1^3}{3} + 2v_0 v_1 v_2 - 20\varkappa v_1\vartheta = 0,\\
(\Omega(\zeta))^4 : 6\kappa v_2 + v_1^2 v_2 + v_0 v_2^2 - 120\varkappa v_2\vartheta = 0,\\
(\Omega(\zeta))^5 : -24\varkappa v_1 + v_1 v_2^2 = 0,\\
(\Omega(\zeta))^6 : -120\varkappa v_2 + \frac{v_2^3}{3} = 0.
\end{cases}$$

The analytical solution of purposed parameters is shown by $\Psi_{1,i,j}$. The equation itself will be presented by the first subscript [1], the family by the second subscript [i], and the method's solution by

the third subscript [j]. Using Mathematica software, the algebraic equation explained above yields the following families:

Family 1: when the parameters are taken as:

$$v_0 = \frac{\sqrt{\kappa} - 20\sqrt{10}\varkappa\vartheta}{10\sqrt{\varkappa}}, v_1 = 0, v_2 = \pm 6\sqrt{10\varkappa}, C = \frac{-\kappa^2 + 10\tau\varkappa + 720\varkappa^2\rho - 240\varkappa^2\vartheta^2}{10\varkappa},$$

$$D = \frac{\sqrt{10}\kappa^3 + 720\sqrt{10}\kappa\varkappa^2\rho + 14400\sqrt{10}\varkappa^3\rho\vartheta - 240\sqrt{10}\kappa\varkappa^2\vartheta^2 - 3200\sqrt{10}\varkappa^3\vartheta^3}{150\varkappa^{\frac{2}{3}}}.$$

Using Eqs. (9), (6) and v_0, v_1, v_2 with $\zeta = r - \tau t$, the solutions listed below are constructed:

Case I: When $\vartheta > 0$ and $\rho = 0$, then

$$\Psi^{\pm}_{1,1,1}(r,t) = \frac{\sqrt{\kappa} - 20\sqrt{10}\varkappa\vartheta}{10\sqrt{\varkappa}} \pm 6\sqrt{10\varkappa}\left(\sqrt{-mn\vartheta} \quad sech_{mn}\left(\sqrt{\vartheta}\zeta\right)\right)^2,$$

$$\Psi^{\pm}_{1,1,2}(r,t) = \frac{\sqrt{\kappa} - 20\sqrt{10}\varkappa\vartheta}{10\sqrt{\varkappa}} \pm 6\sqrt{10\varkappa}\left(\sqrt{mn\vartheta} \quad csch_{mn}\left(\sqrt{\vartheta}\zeta\right)\right)^2.$$

Case II: When $\vartheta < 0$ and $\rho = 0$, then

$$\Psi^{\pm}_{1,1,3}(r,t) = \frac{\sqrt{\kappa} - 20\sqrt{10}\varkappa\vartheta}{10\sqrt{\varkappa}} \pm 6\sqrt{10\varkappa}\left(\sqrt{-mn\vartheta} \quad sec_{mn}\left(\sqrt{-\vartheta}\zeta\right)\right)^2,$$

$$\Psi^{\pm}_{1,1,4}(r,t) = \frac{\sqrt{\kappa} - 20\sqrt{10}\varkappa\vartheta}{10\sqrt{\varkappa}} \pm 6\sqrt{10\varkappa}\left(\sqrt{-mn\vartheta} \quad csc_{mn}\left(\sqrt{-\vartheta}zeta\right)\right)^2.$$

Case III: When $\vartheta < 0$ and $\rho = \frac{\vartheta^2}{4}$, then

$$\Psi^{\pm}_{1,1,5}(r,t) = \frac{\sqrt{\kappa} - 20\sqrt{10}\varkappa\vartheta}{10\sqrt{\varkappa}} \pm 6\sqrt{10\varkappa}\left(\sqrt{\frac{-\vartheta}{2}} \quad tanh_{mn}\left(\sqrt{\frac{-\vartheta}{2}}\zeta\right)\right)^2,$$

$$\Psi^{\pm}_{1,1,6}(r,t) = \frac{\sqrt{\kappa} - 20\sqrt{10}\varkappa\vartheta}{10\sqrt{\varkappa}} \pm 6\sqrt{10\varkappa}\left(\sqrt{\frac{-\vartheta}{2}} coth_{mn}\left(\sqrt{\frac{-\vartheta}{2}}\zeta\right)\right)^2,$$

$$\Psi^{\pm}_{1,1,7}(r,t) = \frac{\sqrt{\kappa} - 20\sqrt{10}\varkappa\vartheta}{10\sqrt{\varkappa}} \pm 6\sqrt{10\varkappa}\left(\sqrt{\frac{-\vartheta}{2}}\left(tanh_{mn}\left(\sqrt{-2\vartheta}\zeta\right) \pm \iota\sqrt{mn} \quad sech_{mn}\left(\sqrt{-2\vartheta}\zeta\right)\right)\right)^2,$$

$$\Psi^{\pm}_{1,1,8}(r,t) = \frac{\sqrt{\kappa} - 20\sqrt{10}\varkappa\vartheta}{10\sqrt{\varkappa}} \pm 6\sqrt{10\varkappa}\left(\sqrt{\frac{-\vartheta}{2}}\left(coth_{mn}\left(\sqrt{-2\vartheta}\zeta\right) \pm \iota\sqrt{mn} \quad csch_{mn}\left(\sqrt{-2\vartheta}\zeta\right)\right)\right)^2,$$

$$\Psi^{\pm}_{1,1,9}(r,t) = \frac{\sqrt{\kappa} - 20\sqrt{10}\varkappa\vartheta}{10\sqrt{\varkappa}} \pm 6\sqrt{10\varkappa}\left(\sqrt{\frac{-\vartheta}{8}}\left(tanh_{mn}\left(\sqrt{\frac{-\vartheta}{8}}\zeta\right) + coth_{mn}\left(\sqrt{\frac{-\vartheta}{8}}\zeta\right)\right)\right)^2.$$

Case IV: When $\vartheta > 0$ and $\rho = \frac{\vartheta^2}{4}$, then

$$\Psi^{\pm}_{1,1,10}(r,t) = \frac{\sqrt{\kappa} - 20\sqrt{10}\varkappa\vartheta}{10\sqrt{\varkappa}} \pm 6\sqrt{10\varkappa}\left(\sqrt{\frac{\vartheta}{2}} \quad tan_{mn}\left(\sqrt{\frac{\vartheta}{2}}\zeta\right)\right)^2,$$

$$\Psi^{\pm}_{1,1,11}(r,t) = \frac{\sqrt{\kappa} - 20\sqrt{10}\varkappa\vartheta}{10\sqrt{\varkappa}} \pm 6\sqrt{10\varkappa}\left(\sqrt{\frac{\vartheta}{2}} \quad cot_{mn}\left(\sqrt{\frac{-\vartheta}{2}}\zeta\right)\right)^2,$$

$$\Psi^{\pm}_{1,1,12}(r,t) = \frac{\sqrt{\kappa} - 20\sqrt{10}\varkappa\vartheta}{10\sqrt{\varkappa}} \pm 6\sqrt{10\varkappa}\left(\sqrt{\frac{\vartheta}{2}}\left(tan_{mn}\left(\sqrt{2\vartheta}\zeta\right) \pm \iota\sqrt{mn} \quad sec_{mn}\left(\sqrt{2\vartheta}\zeta\right)\right)\right)^2,$$

$$\Psi^{\pm}_{1,1,13}(r,t) = \frac{\sqrt{\kappa} - 20\sqrt{10}\varkappa\vartheta}{10\sqrt{\varkappa}} \pm 6\sqrt{10\varkappa}\left(\sqrt{\frac{\vartheta}{2}}\left(cot_{mn}\left(\sqrt{2\vartheta}\zeta\right) \pm \iota\sqrt{mn} \quad csc_{mn}\left(\sqrt{2\vartheta}\zeta\right)\right)\right)^2,$$

$$\Psi^{\pm}_{1,1,14}(r,t) = \frac{\sqrt{\kappa} - 20\sqrt{10}\varkappa\vartheta}{10\sqrt{\varkappa}} \pm 6\sqrt{10\varkappa}\left(\sqrt{\frac{\vartheta}{8}}\left(tan_{mn}\left(\sqrt{\frac{\vartheta}{8}}\zeta\right) + cot_{mn}\left(\sqrt{\frac{\vartheta}{8}}\zeta\right)\right)\right)^2.$$

Family 2: When the parameters are taken as:

$$v_0 = \pm\sqrt{\frac{2\varkappa}{5}}\vartheta, v_1 = \pm\sqrt{6(-\kappa + 22\varkappa\vartheta)}, v_2 = \pm 6\sqrt{10\varkappa}, C = \frac{1}{5}(5\tau + 60\varkappa\rho - 5\kappa\vartheta + 3\varkappa\vartheta^2),$$

$$D = \frac{1}{75}(900\sqrt{10\varkappa}\kappa\rho - 3780\sqrt{10}\varkappa^{\frac{3}{2}}\rho\vartheta + 15\sqrt{10\varkappa}\kappa\vartheta^2 - 11\sqrt{10}\varkappa^{\frac{3}{2}}\vartheta^3).$$

Using Eq. (9), Eq. (6) and v_0, v_1, v_2 with $\zeta = r - \tau t$, the solutions listed below are constructed:

Case I: When $\vartheta > 0$ and $\rho = 0$, then

$$\Psi^{\pm}_{1,2,1}(r,t) = \sqrt{\frac{2\varkappa}{5}}\vartheta \pm \sqrt{6(-\kappa + 22\varkappa\vartheta)}\sqrt{-mn\vartheta}\ sech_{mn}\left(\sqrt{\vartheta}\zeta\right) \pm 6\sqrt{10\varkappa}\left(\sqrt{-mn\vartheta}\ sech_{mn}\left(\sqrt{\vartheta}\zeta\right)\right)^2,$$

$$\Psi^{\pm}_{1,2,2}(r,t) = \sqrt{\frac{2\varkappa}{5}}\vartheta \pm \sqrt{6(-\kappa + 22\varkappa\vartheta)}\left(\sqrt{mn\vartheta} \quad csch_{mn}\left(\sqrt{\vartheta}\zeta\right)\right) \pm 6\sqrt{10\varkappa}\left(\sqrt{mn\vartheta} \quad csch_{mn}\left(\sqrt{\vartheta}\zeta\right)\right)^2.$$

Case II: When $\vartheta < 0$ and $\rho = 0$, then

$$\Psi^{\pm}_{1,2,3}(r,t) = \sqrt{\frac{2\varkappa}{5}}\vartheta \pm \sqrt{6(-\kappa + 22\varkappa\vartheta)}\left(\sqrt{-mn\vartheta}sec_{mn}\left(\sqrt{-\vartheta}\zeta\right)\right)$$
$$\pm 6\sqrt{10\varkappa}\left(\sqrt{-mn\vartheta}sec_{mn}\left(\sqrt{-\vartheta}\zeta\right)\right)^2,$$

$$\Psi^{\pm}_{1,2,4}(r,t) = \sqrt{\frac{2\varkappa}{5}}\vartheta \pm \sqrt{6(-\kappa + 22\varkappa\vartheta)}\left(\sqrt{-mn\vartheta} \quad csc_{mn}\left(\sqrt{-\vartheta}\zeta\right)\right)$$
$$\pm 6\sqrt{10\varkappa}\left(\sqrt{-mn\vartheta} \quad csc_{mn}\left(\sqrt{-\vartheta}\zeta\right)\right)^2.$$

Case III: When $\vartheta < 0$ and $\rho = \frac{\vartheta^2}{4}$, then

$$\Psi^{\pm}_{1,2,5}(r,t) = \sqrt{\frac{2\varkappa}{5}}\vartheta \pm \sqrt{6(-\kappa+22\varkappa\vartheta)}\left(\sqrt{\frac{-\vartheta}{2}}\ tanh_{mn}\left(\sqrt{\frac{-\vartheta}{2}}\zeta\right)\right)$$
$$\pm 6\sqrt{10\varkappa}\left(\sqrt{\frac{-\vartheta}{2}}\ tanh_{mn}\left(\sqrt{\frac{-\vartheta}{2}}\zeta\right)\right)^2,$$

$$\Psi^{\pm}_{1,2,6}(r,t) = \sqrt{\frac{2\varkappa}{5}}\vartheta \pm \sqrt{6(-\kappa+22\varkappa\vartheta)}\left(\sqrt{\frac{-\vartheta}{2}}\quad coth_{mn}\left(\sqrt{\frac{-\vartheta}{2}}\zeta\right)\right)$$
$$\pm 6\sqrt{10\varkappa}\left(\sqrt{\frac{-\vartheta}{2}}\quad coth_{mn}\left(\sqrt{\frac{-\vartheta}{2}}\zeta\right)\right)^2,$$

$$\Psi^{\pm}_{1,2,7}(r,t) = \sqrt{\frac{2\varkappa}{5}}\vartheta \pm \sqrt{6(-\kappa+22\varkappa\vartheta)}\left(\sqrt{\frac{-\vartheta}{2}}\left(tanh_{mn}(\sqrt{-2\vartheta}\zeta) \pm \iota\sqrt{mn}\quad sech_{mn}\left(\sqrt{-2\vartheta}\zeta\right)\right)\right)$$
$$\pm 6\sqrt{10\varkappa}\left(\sqrt{\frac{-\vartheta}{2}}\left(tanh_{mn}\left(\sqrt{-2\vartheta}\zeta\right) \pm \iota\sqrt{mn}\quad sech_{mn}\left(\sqrt{-2\vartheta}\zeta\right)\right)\right)^2,$$

$$\Psi^{\pm}_{1,2,8}(r,t) = \sqrt{\frac{2\varkappa}{5}}\vartheta \pm \sqrt{6(-\kappa+22\varkappa\vartheta)}\left(\sqrt{\frac{-\vartheta}{2}}\left(coth_{mn}\left(\sqrt{-2\vartheta}\zeta\right) \pm \iota\sqrt{mn}\quad csch_{mn}\left(\sqrt{-2\vartheta}\zeta\right)\right)\right)$$
$$\pm 6\sqrt{10\varkappa}\left(\sqrt{\frac{-\vartheta}{2}}\left(coth_{mn}\left(\sqrt{-2\vartheta}\zeta\right) \pm \iota\sqrt{mn}\quad csch_{mn}\left(\sqrt{-2\vartheta}\zeta\right)\right)\right)^2,$$

$$\Psi^{\pm}_{1,2,9}(r,t) = \sqrt{\frac{2\varkappa}{5}}\vartheta \pm \sqrt{6(-\kappa+22\varkappa\vartheta)}\left(\sqrt{\frac{-\vartheta}{8}}\left(tanh_{mn}\left(\sqrt{\frac{-\vartheta}{8}}\zeta\right) + coth_{mn}\left(\sqrt{\frac{-\vartheta}{8}}\zeta\right)\right)\right)$$
$$\pm 6\sqrt{10\varkappa}\left(\sqrt{\frac{-\vartheta}{8}}\left(tanh_{mn}\left(\sqrt{\frac{-\vartheta}{8}}\zeta\right) + coth_{mn}\left(\sqrt{\frac{-\vartheta}{8}}\zeta\right)\right)\right)^2.$$

Case IV: When $\vartheta > 0$ and $\rho = \frac{\vartheta^2}{4}$, then

$$\Psi^{\pm}_{1,2,10}(r,t) = \sqrt{\frac{2\varkappa}{5}}\vartheta \pm \sqrt{6(-\kappa+22\varkappa\vartheta)}\left(\sqrt{\frac{\vartheta}{2}}\quad tan_{mn}\left(\sqrt{\frac{\vartheta}{2}}\zeta\right)\right) \pm 6\sqrt{10\varkappa}(\sqrt{\frac{\vartheta}{2}}\quad tan_{mn}(\sqrt{\frac{\vartheta}{2}}\zeta))^2,$$

$$\Psi^{\pm}_{1,2,11}(r,t) = \sqrt{\frac{2\varkappa}{5}}\vartheta \pm \sqrt{6(-\kappa+22\varkappa\vartheta)}\left(\sqrt{\frac{\vartheta}{2}}\quad cot_{mn}\left(\sqrt{\frac{-\vartheta}{2}}\zeta\right)\right) \pm 6\sqrt{10\varkappa}\left(\sqrt{\frac{\vartheta}{2}}\quad cot_{mn}\left(\sqrt{\frac{-\vartheta}{2}}\zeta\right)\right)^2,$$

$$\Psi^{\pm}_{1,2,12}(r,t) = \sqrt{\frac{2\varkappa}{5}}\vartheta \pm \sqrt{6(-\kappa+22\varkappa\vartheta)}\left(\sqrt{\frac{\vartheta}{2}}\left(tan_{mn}\left(\sqrt{2\vartheta}\zeta\right) \pm \iota\sqrt{mn}\quad sec_{mn}\left(\sqrt{2\vartheta}\zeta\right)\right)\right)$$
$$\pm 6\sqrt{10\varkappa} + \left(\sqrt{\frac{\vartheta}{2}}\left(tan_{mn}\left(\sqrt{2\vartheta}\zeta\right) \pm \iota\sqrt{mn}\quad sec_{mn}\left(\sqrt{2\vartheta}\zeta\right)\right)\right)^2,$$

$$\Psi^{\pm}_{1,2,13}(r,t) = \sqrt{\frac{2\varkappa}{5}}\vartheta \pm \sqrt{6(-\kappa+22\varkappa\vartheta)}\left(\sqrt{\frac{\vartheta}{2}}\left(cot_{mn}\left(\sqrt{2\vartheta}\zeta\right) \pm \iota\sqrt{mn}\quad csc_{mn}\left(\sqrt{2\vartheta}\zeta\right)\right)\right)$$
$$\pm 6\sqrt{10\varkappa}\left(\sqrt{\frac{\vartheta}{2}}\left(cot_{mn}\left(\sqrt{2\vartheta}\zeta\right) \pm \iota\sqrt{mn}\quad csc_{mn}\left(\sqrt{2\vartheta}\zeta\right)\right)\right)^2,$$
$$\Psi^{\pm}_{1,2,14}(r,t) = \sqrt{\frac{2\varkappa}{5}}\vartheta \pm \sqrt{6(-\kappa+22\varkappa\vartheta)}\left(\sqrt{\frac{\vartheta}{8}}\left(tan_{mn}\left(\sqrt{\frac{\vartheta}{8}}\zeta\right)+cot_{mn}\left(\sqrt{\frac{\vartheta}{8}}\zeta\right)\right)\right)$$
$$\pm 6\sqrt{10\varkappa}\left(\sqrt{\frac{\vartheta}{8}}\left(tan_{mn}\left(\sqrt{\frac{\vartheta}{8}}\zeta\right)+cot_{mn}\left(\sqrt{\frac{\vartheta}{8}}\zeta\right)\right)\right)^2.$$

3.2 Modified Benjamin-Bona-Mahony Equation

In this section, we utilize the SSE method to mBBM equation. Employing the wave transformation $\zeta = \varepsilon(r-\varrho t)$ and $\Phi(r,t) = \Phi(\zeta)$ holds Eq. (2) into ODE, where parameter ε controls the scaling of the wave variable ζ. The resulting equation integrated twice, we get

$$\varrho\varepsilon\theta\Phi'' - \frac{1}{3}\Phi^3 + (\varrho-1)\Phi - \gamma + C\Phi + D = 0, \tag{10}$$

where C and D are constants. Following the highest order derivative term Φ'' and the highest order nonlinear term Φ^3 being balanced, yields $3L = L+2$, $L=1$ are achieved. Therefore, employing the SSE approach, the solution to Eq. (10) has the following form:

$$\Phi(\zeta) = v_0 + v_1\Omega(\zeta), \tag{11}$$

where v_0, v_1 are constants. Substitute Eq. (10), Eq. (11) into Eq. (6).

$$-\gamma+D-v_0+Cv_0+\varrho v_0-\frac{{v_0}^3}{3}-v_1\Omega+Cv_1\Omega+\varrho v_1\Omega-{v_0}^2v_1\Omega+\theta\varrho^2v_1\vartheta\,\Omega-v_0{v_1}^2\Omega^2+2\theta\varrho^2v_1\Omega^3-\frac{1}{3}{v_1}^3\Omega^3. \tag{12}$$

By taking the polynomial in the form of $\Omega^s(\zeta)$ and equal its powers to zero. We get

$$\begin{cases}(\Omega(\zeta))^0 : -\gamma + D + (C-1)v_0 + \varrho v_0 - \frac{{v_0}^3}{3} = 0,\\ (\Omega(\zeta))^1 : -v_1 + Cv_1 + \varrho v_1 - v-0^2v_1 + \theta\varrho^2v_1\vartheta = 0,\\ (\Omega(\zeta))^2 : -v_0{v_1}^2 = 0,\\ (\Omega(\zeta))^3 : 2\theta\varrho^2v_1 - \frac{{v_1}^3}{3} = 0.\end{cases}$$

The analytical solution of purposed parameters is shown by $\Phi_{2,j}$. The equation itself will be presented by the first subscript [2], and the method's solution by the second subscript [j]. Using Mathematica software, the algebraic equation explained above yields the following parameters:

$$v_0 = 0, v_1 = \pm\sqrt{6\theta}\varrho, C = 1-\varrho-\theta\varrho^2\vartheta, D = \gamma.$$

Using Eqs. (11), (6) and v_0, v_1 with $\zeta = \varepsilon(r-\varrho t)$, the solutions listed below are constructed:

Case I: When $\vartheta > 0$ and $\rho = 0$, then

$$\Phi_{2,1}^{\pm}(r,t) = \pm\sqrt{6\theta}\varrho\left(\sqrt{-mn\vartheta}\quad sech_{mn}\left(\sqrt{\vartheta}\zeta\right)\right),$$

$$\Phi_{2,2}^{\pm}(r,t) = \pm\sqrt{6\theta}\varrho\left(\sqrt{mn\vartheta}\quad csch_{mn}\left(\sqrt{\vartheta}\zeta\right)\right).$$

Case II: When $\vartheta < 0$ and $\rho = 0$, then

$$\Phi_{2,3}^{\pm}(r,t) = \pm\sqrt{6\theta}\varrho\left(\sqrt{-mn\vartheta}\quad sec_{mn}\left(\sqrt{-\vartheta}\zeta\right)\right),$$

$$\Phi_{2,4}^{\pm}(r,t) = \pm\sqrt{6\theta}\varrho\left(\sqrt{-mn\vartheta}\quad csc_{mn}\left(\sqrt{-\vartheta}\zeta\right)\right).$$

Case III: When $\vartheta < 0$ and $\rho = \dfrac{\vartheta^2}{4}$, then

$$\Phi_{2,5}^{\pm}(r,t) = \pm\sqrt{6\theta}\varrho\left(\sqrt{\frac{-\vartheta}{2}}\ tanh_{mn}\left(\sqrt{\frac{-\vartheta}{2}}\zeta\right)\right),$$

$$\Phi_{2,6}^{\pm}(r,t) = \pm\sqrt{6\theta}\varrho\left(\sqrt{\frac{-\vartheta}{2}}\quad coth_{mn}\left(\sqrt{\frac{-\vartheta}{2}}\zeta\right)\right),$$

$$\Phi_{2,7}^{\pm}(r,t) = \pm\sqrt{6\theta}\varrho\left(\sqrt{\frac{-\vartheta}{2}}\left(tanh_{mn}(\sqrt{-2\vartheta}\zeta) \pm \iota\sqrt{mn}\quad sech_{mn}\left(\sqrt{-2\vartheta}\zeta\right)\right)\right),$$

$$\Phi_{2,8}^{\pm}(r,t) = \pm\sqrt{6\theta}\varrho\left(\sqrt{\frac{-\vartheta}{2}}\left(coth_{mn}(\sqrt{-2\vartheta}\zeta) \pm \iota\sqrt{mn}\quad csch_{mn}\left(\sqrt{-2\vartheta}\zeta\right)\right)\right),$$

$$\Phi_{2,9}^{\pm}(r,t) = \pm\sqrt{6\theta}\varrho\left(\sqrt{\frac{-\vartheta}{8}}\left(tanh_{mn}\left(\sqrt{\frac{-\vartheta}{8}}\zeta\right) + coth_{mn}\left(\sqrt{\frac{-\vartheta}{8}}\zeta\right)\right)\right).$$

Case IV: When $\vartheta > 0$ and $\rho = \dfrac{\vartheta^2}{4}$, then

$$\Phi_{2,10}^{\pm}(r,t) = \pm\sqrt{6\theta}\varrho\left(\sqrt{\frac{\vartheta}{2}}\quad tan_{mn}\left(\sqrt{\frac{\vartheta}{2}}\zeta\right)\right),$$

$$\Phi_{2,11}^{\pm}(r,t) = \pm\sqrt{6\theta}\varrho\left(\sqrt{\frac{\vartheta}{2}}\quad cot_{mn}\left(\sqrt{\frac{-\vartheta}{2}}\zeta\right)\right),$$

$$\Phi_{2,12}^{\pm}(r,t) = \pm\sqrt{6\theta}\varrho\left(\sqrt{\frac{\vartheta}{2}}\left(tan_{mn}(\sqrt{2\vartheta}\zeta) \pm \iota\sqrt{mn}\quad sec_{mn}\left(\sqrt{2\vartheta}\zeta\right)\right)\right),$$

$$\Phi_{2,13}^{\pm}(r,t) = \pm\sqrt{6\theta}\varrho\left(\sqrt{\frac{\vartheta}{2}}\left(cot_{mn}(\sqrt{2\vartheta}\zeta) \pm \iota\sqrt{mn}\quad csc_{mn}\left(\sqrt{2\vartheta}\zeta\right)\right)\right),$$

$$\Phi_{2,14}^{\pm}(r,t) = \pm\sqrt{6\theta}\varrho\left(\sqrt{\frac{\vartheta}{8}}\left(tan_{mn}\left(\sqrt{\frac{\vartheta}{8}}\zeta\right) + cot_{mn}\left(\sqrt{\frac{\vartheta}{8}}\zeta\right)\right)\right).$$

4 Graphical Representation

To further support the validity and reliability of the obtained solutions, we have verified each by direct substitution into the original equations, ensuring they satisfy the required conditions. The graphical representations not only illustrate the physical behavior of the solutions but also provide qualitative confirmation of their accuracy. Moreover, the SSE method demonstrates computational efficiency by yielding diverse soliton structures such as bell-shaped, and periodic forms through a relatively straightforward analytical process. This highlights the method's strength in exploring complex nonlinear dynamics in modified evolution equations. These varied soliton profiles reflect the rich dynamical behavior of the system, where the interplay of nonlinearity and dispersion governs wave stability, shape, and evolution. By examining these graphical illustrations, one can observe how different soliton types propagate, interact, and maintain their form, offering deeper insight into the underlying physics. Such visualizations emphasize the dynamical system's capability to model complex wave phenomena in nonlinear media, thus reinforcing the importance of the analytical solutions presented. These profiles include bell-shaped, anti-bell-shaped, M-W periodic-shaped, W-periodic shaped, V-shaped, periodic-shaped solitons, and compactons. A description of the physical properties and behaviors of each figure is given, representing an optical soliton solution. These profiles include bell-shaped, anti-bell-shaped, M-W periodic-shaped, W-periodic shaped, V-shaped, periodic-shaped solitons, and compactons. A description of the physical properties and behaviors of each figure is given, representing an optical soliton solution. The detailed parameter values used to generate each soliton profile are summarized in Table 1. Fig. 1 depicts $3D$ and $2D$ graphs of $\Psi_{1,1,2}(r,t)$ by using these value $\vartheta = 0.1, \tau = 0.5, \kappa = -1, \varkappa = 0.1, m = -1, n = 0.1$ between the range $-10 \leq r \leq 10$, $-10 \leq t \leq 10$ that is dark shape soliton, its soliton has an elevated peak, but this is a restricted wave with a negative peak and also referred to as "anti-bell" solitons. Fig. 2 depicts $3D$ and $2D$ graphs of $\Psi_{1,1,4}(r,t)$ by using these values $\vartheta = -0.3, \tau = 0.5, \kappa = 1, \varkappa = 0.2, m = 0.5, n = 0.1$ between the range $-5 \leq r \leq 5$, $-5 \leq t \leq 5$ that is periodic shape soliton, that can maintan their pattern regularly and transfer energy through the medium. Fig. 3 depicts $3D$ and $2D$ graphs of $\Psi_{1,1,5}(r,t)$ by using these values $\vartheta = -0.1, \tau = 0.3, \kappa = 0.1, \varkappa = 0.2, m = 0.1, n = 0.1$ between the range $-5 \leq r \leq 5$, $-10 \leq t \leq 10$ that is compacton shape soliton, since they behave like particles, it can be used to simulate atoms in systems that are not linear. Fig. 4 depicts $3D$ and $2D$ graphs of $\Psi_{1,1,10}(r,t)$ by using these values $\vartheta = 0.3, \tau = 0.5, \kappa = 0.1, \varkappa = 0.2, m = 0.1, n = 0.4$ between the range $-5 \leq r \leq 5$, $0 \leq t \leq 4$ that is bright-dark soliton, helpful for studying nonlinear behavior since, according to the system, it can be either stable or unstable. Fig. 5 depicts $3D$ and $2D$ graphs of $\Psi_{1,2,1}(r,t)$ by using these values $\vartheta = 0.1, \tau = 0.3, \kappa = 0.5, \varkappa = 0.3, m = 0.5, n = 0.1$ between the range $-5 \leq r \leq 5$, $-10 \leq t \leq 10$ that is bright shape soliton. Fig. 6 depicts $3D$ and $2D$ graphs of $\Psi_{1,2,3}(r,t)$ by using these values $\vartheta = -0.1, \tau = 1, \kappa = 0.05, \varkappa = 0.1, m = 2, n = 1$ between the range $-10 \leq r \leq 10$, $-10 \leq t \leq 10$ that is W-periodic shape soliton, it shows periodic wave that repeat their pattern in the specific W form. Fig. 7 depicts $3D$ and $2D$ graphs of $\Psi_{1,2,6}(r,t)$ by using these values $\vartheta = -0.01, \tau = -0.5, \kappa = 0.2, \varkappa = 0.3, m = 0.2, n = 0.3$ between the range $-2 \leq r \leq 2$,$-2 \leq t \leq 1$ that is anti-compacton soliton. Fig. 8 depicts $3D$ and $2D$ graphs of $\Psi_{1,2,12}(r,t)$ by using these values $\vartheta = 0.3, \tau = 0.5, \kappa = 0.1, \varkappa = 0.1, m = 0.1, n = 0.2$ between the range $-10 \leq r \leq 10$, $0 \leq t \leq 2$ that is M-W periodic shape soliton that can show phenomena like periodic waves. Fig. 9 depicts $3D$ and $2D$ graphs of $\Phi_{2,1}(r,t)$ by using these values $\vartheta = 0.1, \varepsilon = 0.5, \theta = 1, \varrho = 0.5, m = 1, n = 1$ between the range $-20 \leq r \leq 20$, $-20 \leq t \leq 20$ that is bell shape soliton, it has a long lifetime and are essential for interpreting many physical phenomena. Fig. 10 depicts $3D$ and $2D$ graphs of $\Phi_{2,3}(r,t)$ by using these values $\vartheta = -0.2, \varepsilon = 0.7, \theta = 1, \varrho = 0.5, m = 1, n = 0.1$ between the range $-10 \leq r \leq 10$, $-10 \leq t \leq 10$ that is periodic' shape soliton. Fig. 11 depicts $3D$ and $2D$ graphs of $\Phi_{2,14}(r,t)$ by using

these values $\vartheta = 1, \varepsilon = -0.5, \theta = 1, \varrho = -0.5, m = 0.8, n = 0.2$ between the range $-5 \leq r \leq 5$, $-5 \leq t \leq 5$ that is V-shape soliton, They constitute V-shaped, exclusive waves that can behave in a dispersive or non-dispersive manner. Considering their distinct shapes and mechanical characteristics, such graphic representations provide deep understanding into the various optical soliton solutions established.

Table 1: Parameter values and types of nonlinear waves from graphical representations

Figure	Key parameters	Wave type
Fig. 1	$\vartheta = 0.1, \tau = 0.5, \kappa = -1,$ $\varkappa = 0.1, m = -1, n = 0.1$	Anti-bell soliton
Fig. 2	$\vartheta = -0.3, \tau = 0.5, \kappa = 1,$ $\varkappa = 0.2, m = 0.5, n = 0.1$	Periodic soliton
Fig. 3	$\vartheta = -0.1, \tau = 0.3, \kappa = 0.1,$ $\varkappa = 0.2, m = 0.1, n = 0.1$	Compacton soliton
Fig. 4	$\vartheta = 0.3, \tau = 0.5, \kappa = 0.1,$ $\varkappa = 0.2, m = 0.1, n = 0.4$	Bright-dark soliton
Fig. 5	$\vartheta = 0.1, \tau = 0.3, \kappa = 0.5,$ $\varkappa = 0.3, m = 0.5, n = 0.1$	Bright soliton
Fig. 6	$\vartheta = -0.1, \tau = 1, \kappa = 0.05,$ $\varkappa = 0.1, m = 2, n = 1$	W-periodic soliton
Fig. 7	$\vartheta = -0.01, \tau = -0.5, \kappa = 0.2,$ $\varkappa = 0.3, m = 0.2, n = 0.3$	Anti-compacton soliton
Fig. 8	$\vartheta = 0.3, \tau = 0.5, \kappa = 0.1,$ $\varkappa = 0.1, m = 0.1, n = 0.2$	M-W periodic soliton
Fig. 9	$\vartheta = 0.1, \varepsilon = 0.5, \theta = 1,$ $\varrho = 0.5, m = 1, n = 1$	Bell-shape soliton
Fig. 10	$\vartheta = -0.2, \varepsilon = 0.7, \theta = 1,$ $\varrho = 0.5, m = 1, n = 0.1$	Periodic soliton
Fig. 11	$\vartheta = 1, \varepsilon = -0.5, \theta = 1,$ $\varrho = -0.5, m = 0.8, n = 0.2$	V-shape soliton

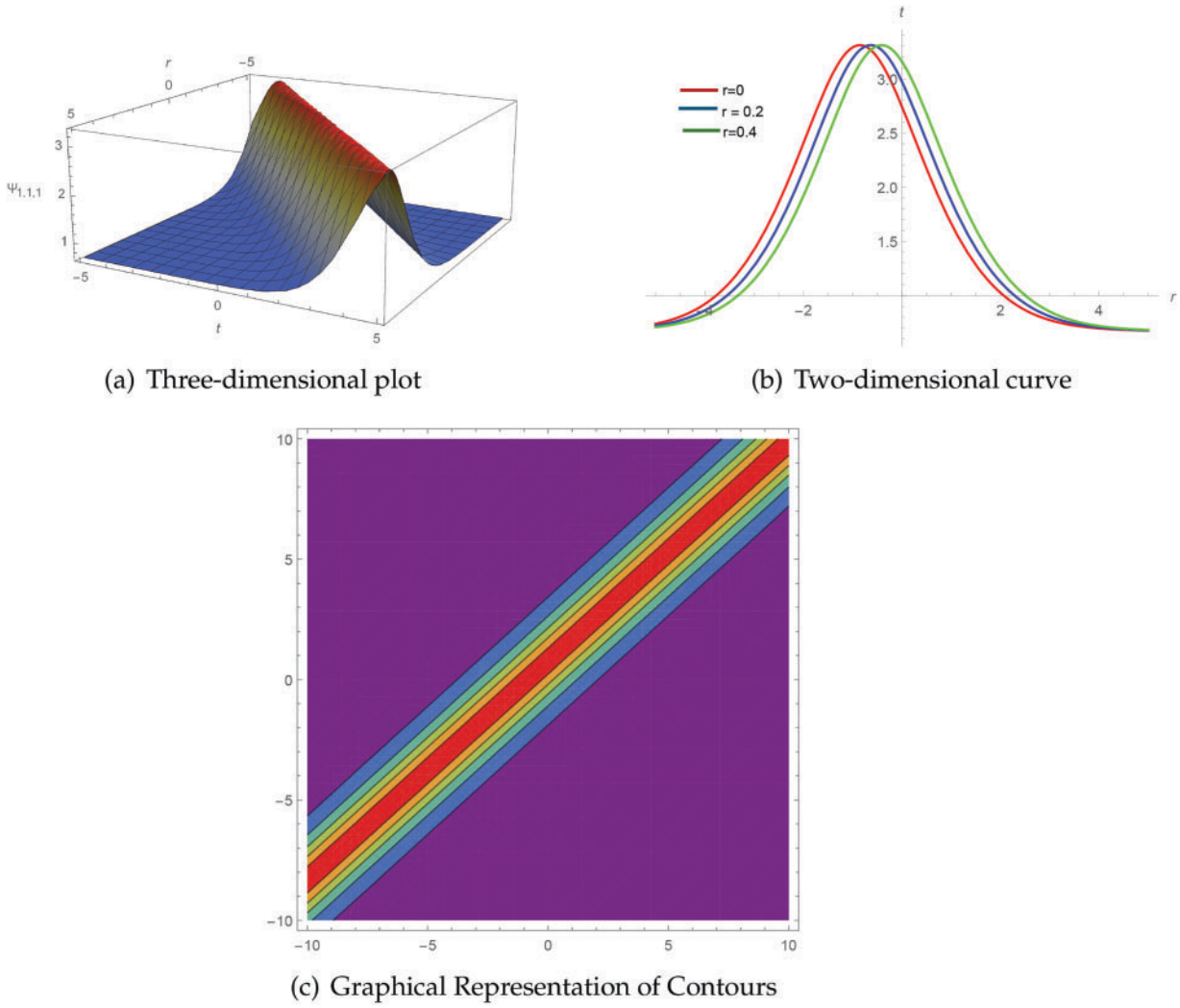

(a) Three-dimensional plot

(b) Two-dimensional curve

(c) Graphical Representation of Contours

Figure 1: Traveling Waveform Solution $\Psi_{1,1,2}(r,t)$ (a) $3D$ graph which is anti-bell shape soliton (b) $2D$ graph (c) Contour Plot, when $\vartheta = 0.1, \tau = 0.5, \kappa = -1, \varkappa = 0.1, m = -1, n = 0.1$

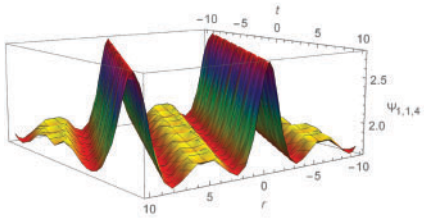

(a) Three-dimensional plot

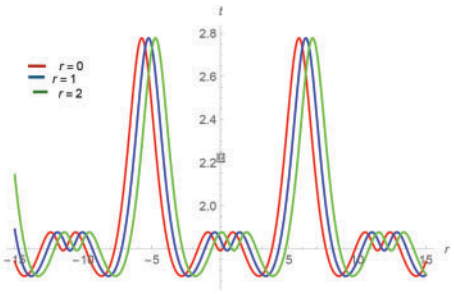

(b) Two-dimensional curve

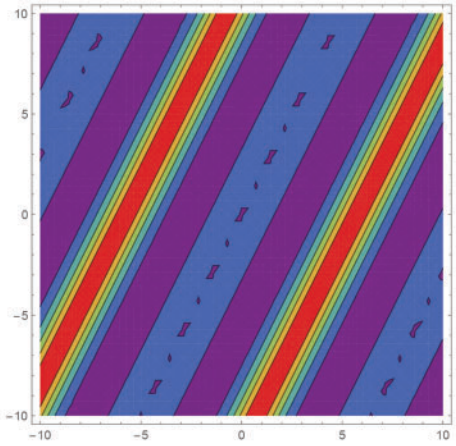

(c) Graphical Representation of Contours

Figure 2: Traveling Waveform Solution $\Psi_{1,1,4}(r,t)$ (a) $3D$ plot which is periodic soliton (b) $2D$ plot (c) Contour plot, when $\vartheta = -0.3, \tau = 0.5, \kappa = 1, \varkappa = 0.2, m = 0.5, n = 0.1$

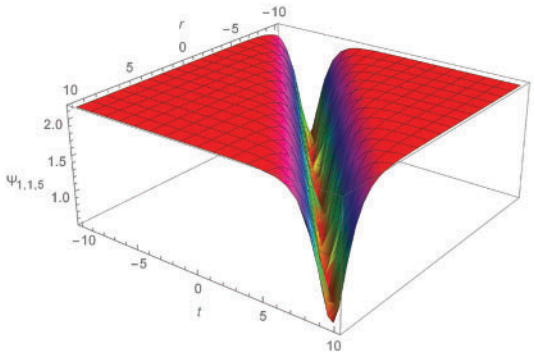

(a) Three-dimensional plot

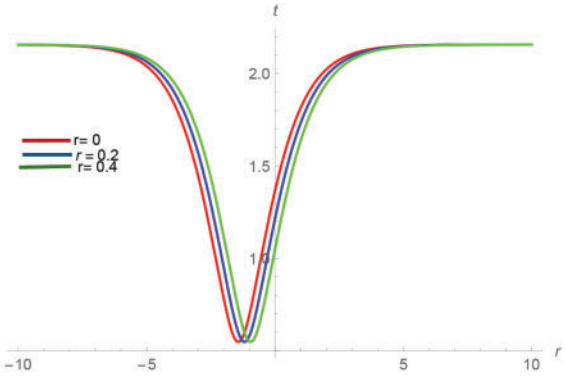

(b) Two-dimensional curve

Figure 3: (Continued)

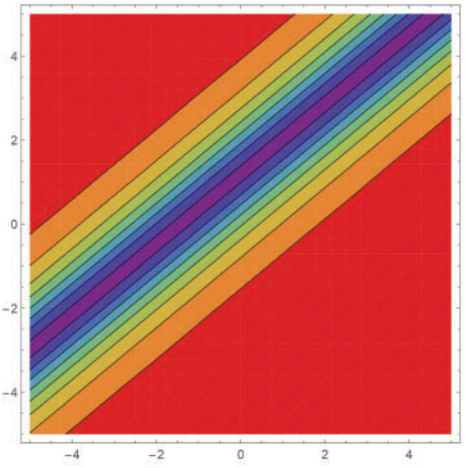

(c) Graphical Representation of Contours

Figure 3: Exact Expression $\Psi_{1,1,5}(r,t)$ (a) $3D$ graph which is compacton shape soliton (b) $2D$ graph (c) Contour Plot, when $\vartheta = -0.1, \tau = 0.3, \kappa = 0.1, \varkappa = 0.2, m = 0.1, n = 0.1$

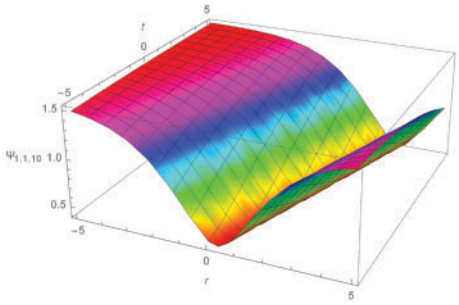

(a) Three-dimensional plot

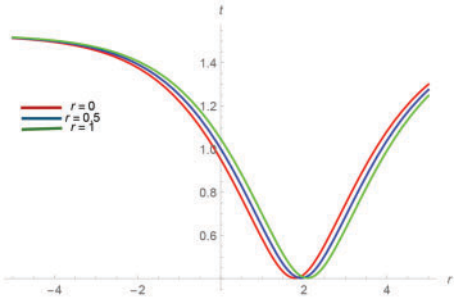

(b) Two-dimensional curve

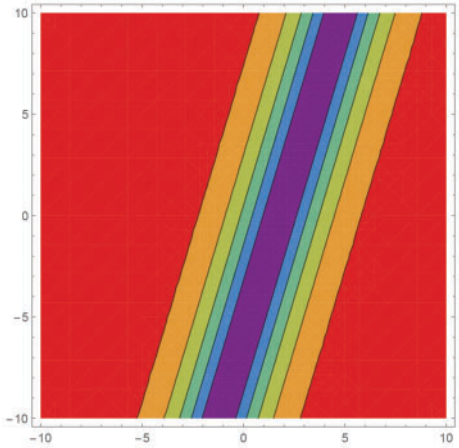

(c) Graphical Representation of Contours

Figure 4: Exact Expression $\Psi_{1,1,10}(r,t)$ (a) $3D$ graph which is bright-dark soliton (b) $2D$ graph (c) Contour Plot, when $\vartheta = 0.3, \tau = 0.5, \kappa = 0.1, \varkappa = 0.2, m = 0.1, n = 0.4$

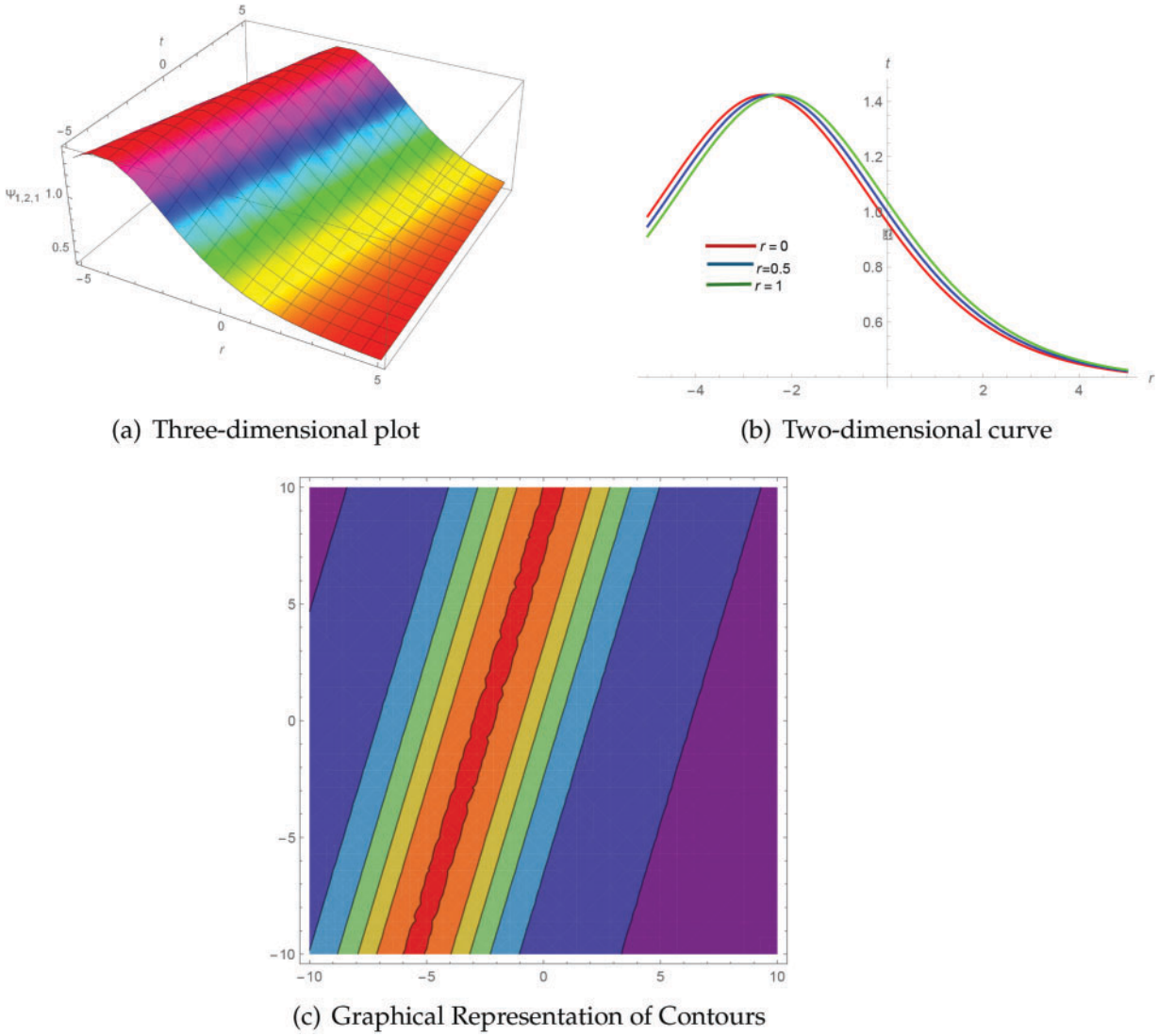

(a) Three-dimensional plot

(b) Two-dimensional curve

(c) Graphical Representation of Contours

Figure 5: Exact Expression $\Psi_{1,2,1}(r,t)$ (a) $3D$ graph which is bright shape soliton (b) $2D$ graph (c) Contour Plot, when $\vartheta = 0.1, \tau = 0.3, \kappa = 0.5, \varkappa = 0.3, m = 0.5, n = 0.1$

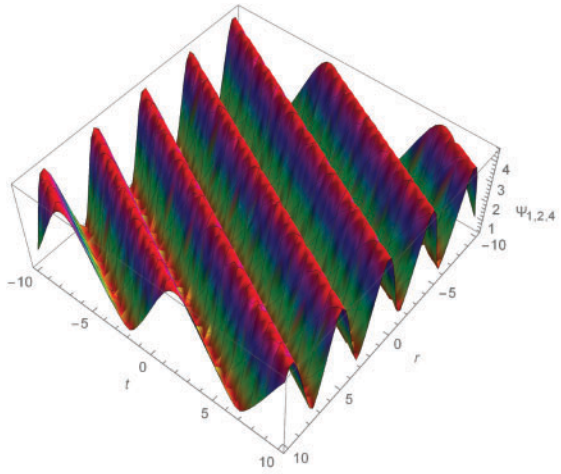

(a) Three-dimensional plot

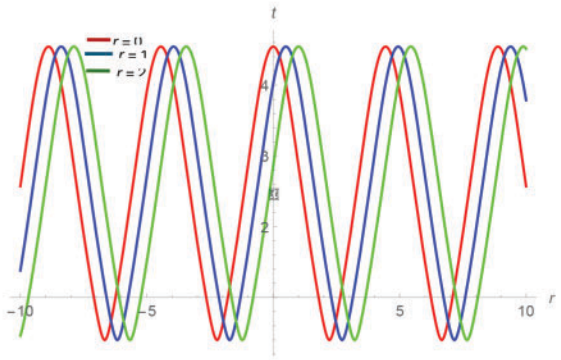

(b) Two-dimensional curve

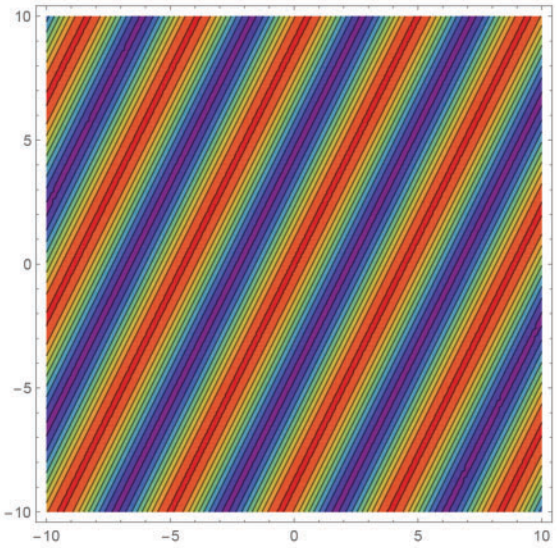

(c) Graphical Representation of Contours

Figure 6: Exact Expression $\Psi_{1,2,3}(r,t)$ (a) $3D$ graph which is W-periodic soliton (b) $2D$ graph (c) Contour Plot, when $\vartheta = -0.1, \tau = 1, \kappa = 0.05, \varkappa = 0.1, m = 2, n = 1$

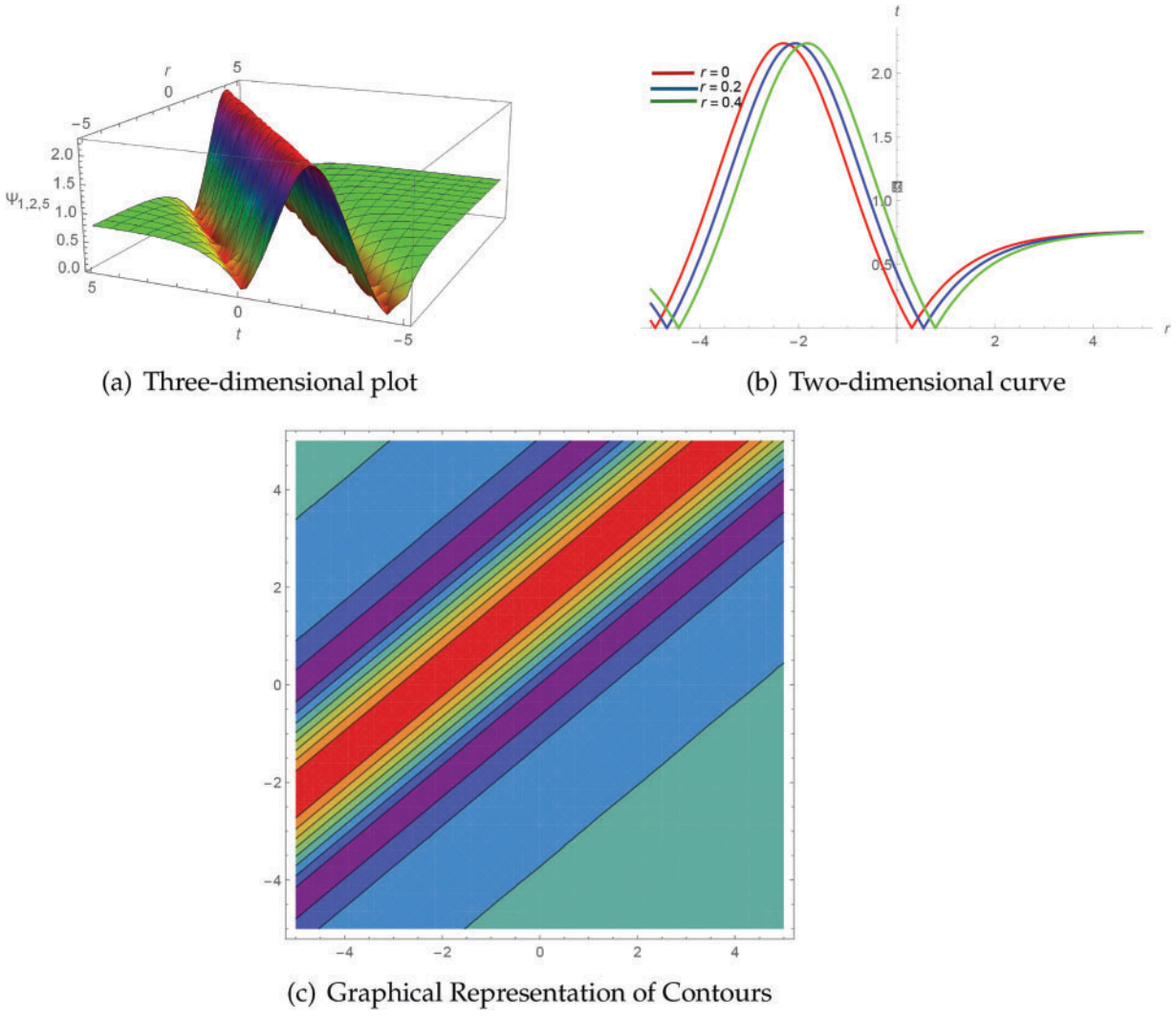

(a) Three-dimensional plot

(b) Two-dimensional curve

(c) Graphical Representation of Contours

Figure 7: Exact Expression $\Psi_{1,2,6}(r,t)$ (a) $3D$ graph which is anti-compacton soliton (b) $2D$ graph (c) Contour Plot, when $\vartheta = -0.01, \tau = -0.5, \kappa = 0.2, \varkappa = 0.3, m = 0.2, n = 0.3$

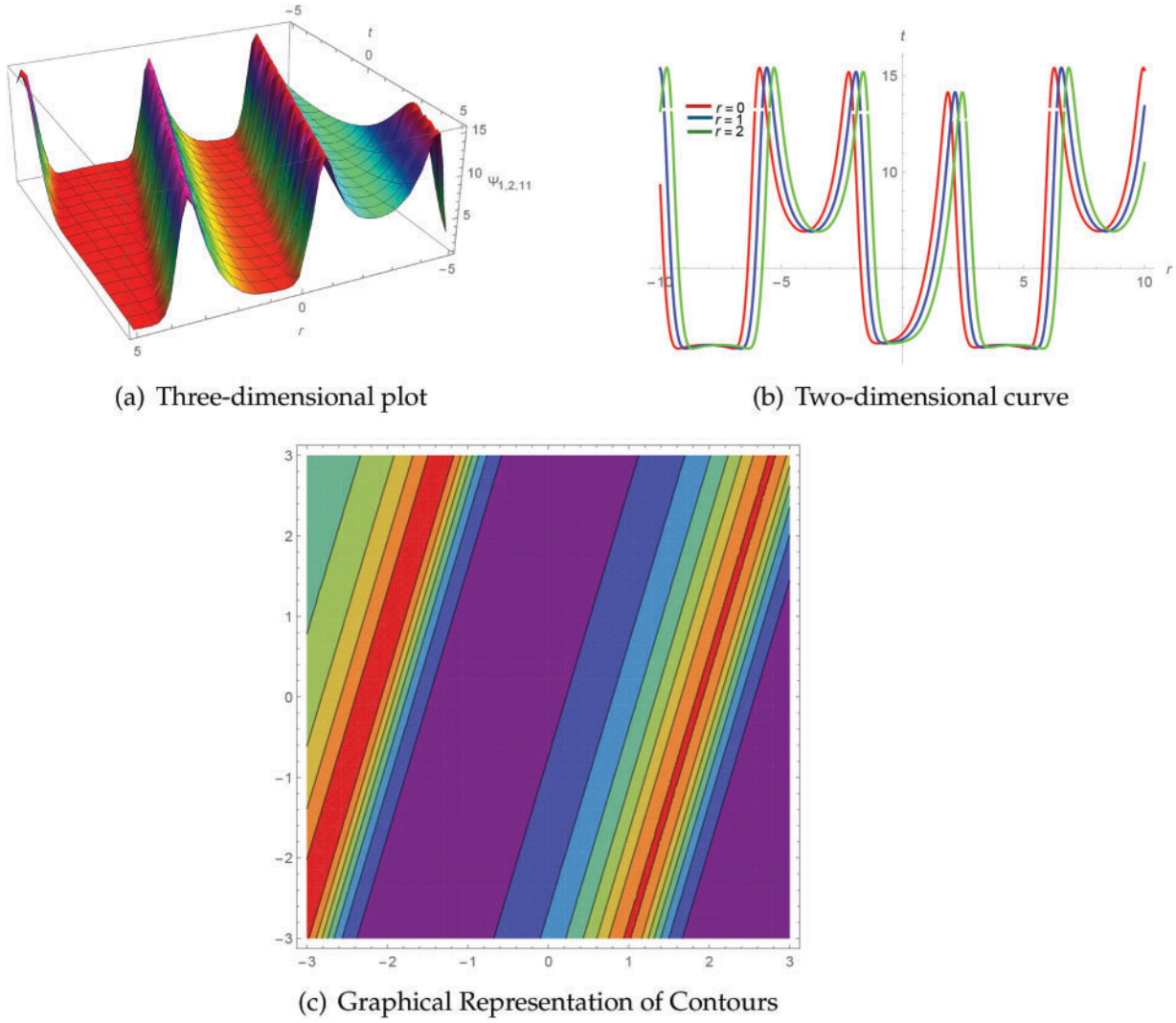

(a) Three-dimensional plot

(b) Two-dimensional curve

(c) Graphical Representation of Contours

Figure 8: Exact Expression $\Psi_{1,2,12}(r,t)$ (a) $3D$ graph which is M-W periodic shape soliton (b) $2D$ graph (c) Contour Plot, when $\vartheta = 0.3, \tau = 0.5, \kappa = 0.1, \varkappa = 0.1, m = 0.1, n = 0.2$

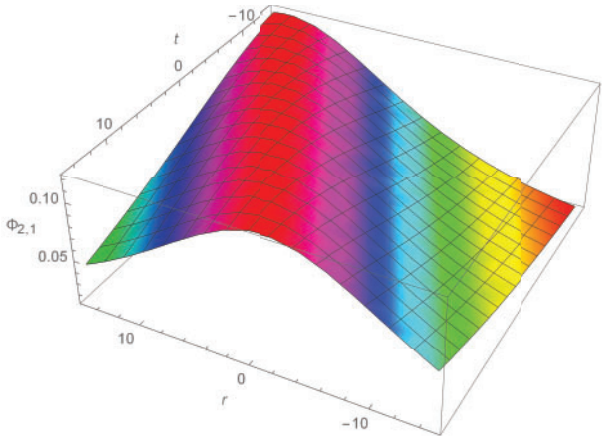

(a) Three-dimensional plot

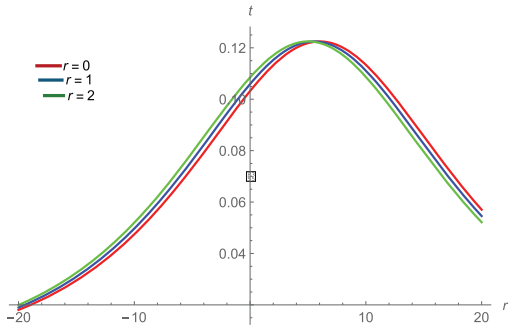

(b) Two-dimensional curve

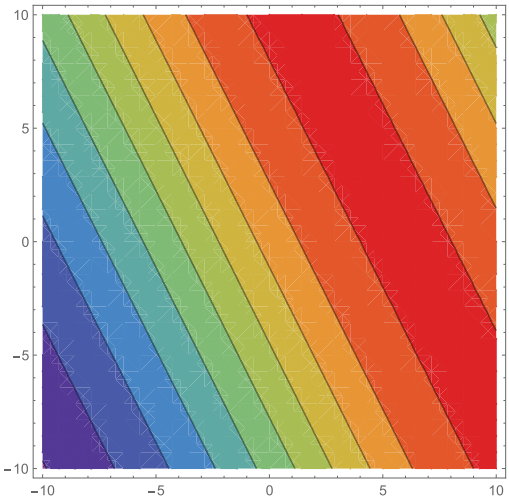

(c) Graphical Representation of Contours

Figure 9: Exact Expression $\Phi_{2,1}(r,t)$ (a) $3D$ graph which is bell shape soliton (b) $2D$ graph (c) Contour Plot, when $\vartheta = 0.1, \varepsilon = 0.5, \theta = 1, \varrho = 0.5, m = 1, n = 1$

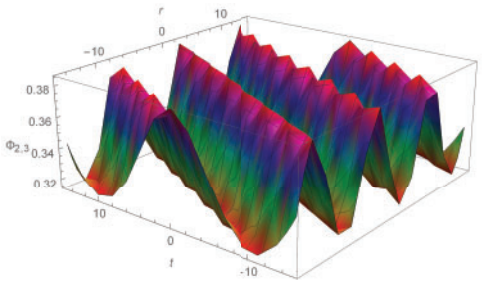

(a) Three-dimensional plot

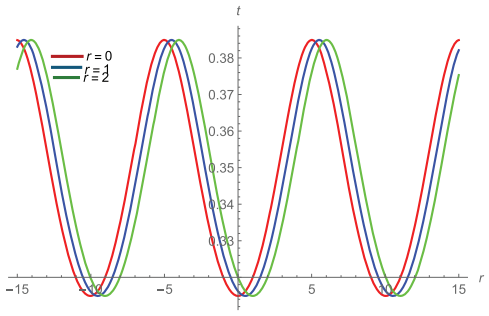

(b) Two-dimensional curve

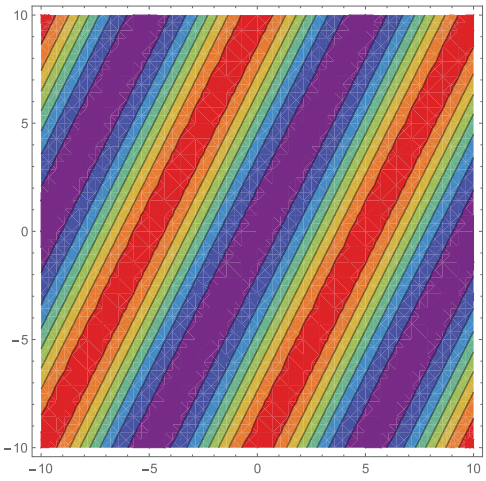

(c) Graphical Representation of Contours

Figure 10: Exact Expression $\Phi_{2,3}(r,t)$ (a) $3D$ graph which is periodic shape soliton (b) $2D$ graph (c) Contour Plot, when $\vartheta = -0.2, \varepsilon = 0.7, \theta = 1, \varrho = 0.5, m = 1, n = 0.1$

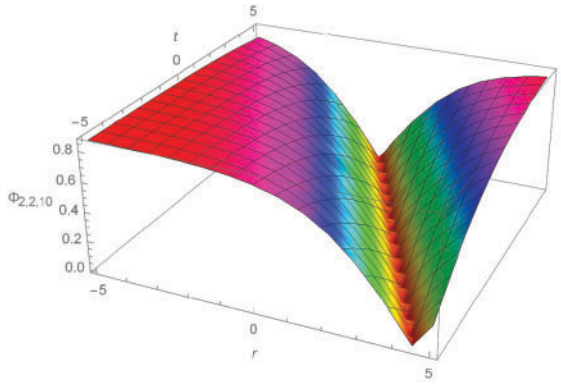

(a) Three-dimensional plot

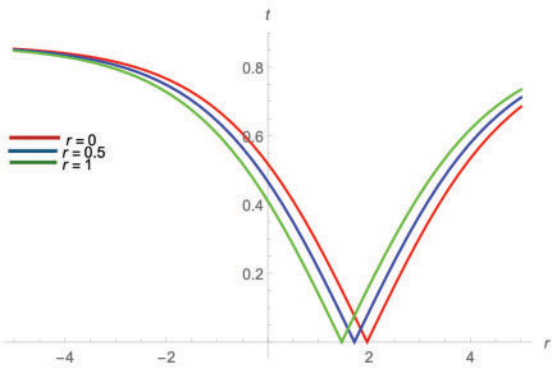

(b) Two-dimensional curve

Figure 11: (Continued)

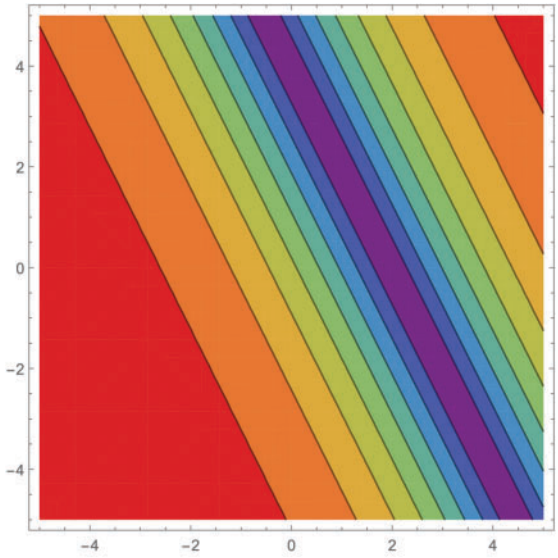

(c) Graphical Representation of Contours

Figure 11: Exact Expression $\Phi_{2,14}(r,t)$ (a) $3D$ graph which is V-shape soliton (b) $2D$ graph (c) Contour Plot, when $\vartheta = 1, \varepsilon = -0.5, \theta = 1, \varrho = -0.5, m = 0.8, n = 0.2$

5 Physical Meaning of the Graphs

The graphs in Figs. 1–11 illustrate key physical properties of solitons, such as stability, localization of energy, and solitary wave behavior. These soliton solutions arise from a balance between nonlinear effects and dispersion, which is fundamental in many nonlinear wave systems. Physically, these solutions model phenomena in diverse fields including water waves, optical fiber communication, plasma physics, and quantum fluids. Different soliton shapes correspond to various wave behaviors:

- **Bell-shaped and bright solitons** represent stable, localized pulses that maintain their form over time.
- **Anti-bell and dark solitons** correspond to localized dips or voids in the wave profile.
- **Periodic and W-shaped solitons** depict repeating wave patterns important for energy transfer in nonlinear media.
- **Compactons** behave like particles and are useful in modeling nonlinear atomic or mechanical systems.
- **V-shaped solitons** show unique dispersive and non-dispersive characteristics relevant to wave interactions.

These soliton structures have wide-ranging applications, including mode-locking in lasers, data transmission in optical fibers, plasma wave dynamics, and biological and quantum systems. The graphical representations therefore not only confirm the mathematical solutions but also provide valuable insight into their physical relevance and potential practical uses.

6 Conclusions

In this study, we have successfully developed and implemented the SSE method to derive a wide variety of optical soliton solutions for the mK and the mBBM equations. The primary contribution of this work lies in the systematic construction of multiple families of exact solutions, including bell-shaped, anti-bell-shaped, W-shaped, M-shaped, and periodic waveforms. These solutions highlight the flexibility and robustness of the SSE method in handling complex nonlinear partial differential equations and capturing diverse nonlinear wave phenomena. The detailed $2D$, $3D$, and contour plots provided offer valuable insights into the physical characteristics and dynamic behaviors of the obtained solitons, which are of great importance in various applied fields such as optical communication systems and fluid mechanics. By extending the library of known exact solutions for the mK and mBBM equations, this research not only advances the theoretical understanding of these nonlinear models but also opens up new avenues for their practical applications. Future work may focus on the experimental validation of these analytical solutions and their numerical simulation under different initial and boundary conditions. Furthermore, the versatility of the SSE method suggests its potential applicability to other nonlinear evolution equations arising in mathematical physics and engineering, thereby contributing to the broader study of nonlinear wave dynamics.

Acknowledgement: Not applicable.

Funding Statement: Not applicable.

Author Contributions: Funding acquisition: Muhammad Abbas, Hadia Khalid Mehmood and Ibrahim Sulaiman Ibrahim. Methodology: Hadia Khalid Mehmood, Muhammad Abbas, Majeed Ahmad Yousif and Pshtiwan Othman Mohammed. Supervision: Dumitru Baleanu and Muhammad Abbas. Visualization: Pshtiwan Othman Mohammed, Majeed Ahmad Yousif and Farah Aini Abdullah. Writing—original draft: Hadia Khalid Mehmood, Majeed Ahmad Yousif and Ibrahim Sulaiman Ibrahim. Writing—review & editing: Dumitru Baleanu, Muhammad Abbas and Pshtiwan Othman Mohammed. All authors reviewed the results and approved the final version of the manuscript.

Availability of Data and Materials: Not applicable.

Ethics Approval: Not applicable.

Conflicts of Interest: The authors declare no conflicts of interest to report regarding the present study.

References

1. Yousif MA, Guirao JLG, Mohammed PO, Chorfi N, Baleanu D. A computational study of time-fractional gas dynamics models by means of conformable finite difference method. AIMS Math. 2024;9(7):19843–58. doi:10.3934/math.2024969.
2. Yousif MA, Agarwal RP, Mohammed PO, Lupas AA, Jan R, Chorfi N. Advanced methods for conformable time-fractional differential equations: logarithmic non-polynomial splines. Axioms. 2024;13(8):551. doi:10.3390/axioms13080551.
3. Rahman M, Assiri TA, Saifullah S, Meraj A, Mei S. Some new optical solitary wave solutions of a third-order dispersive Schrödinger equation with Kerr nonlinearity using an efficient approach associated with the Riccati equation. Optics and Quantum Electron. 2024;56(4):646. doi:10.1007/s11082-023-06208-3.

4. Faridi WA, Tipu GH, Riaz MB, Almetwally MM, Salman A, Ratbay M, et al. Analyzing optical soliton solutions in the Kairat-X equation via a new auxiliary equation method. Opt Quant Electron. 2024;56(8):1317. doi:10.1007/s11082-024-07197-7.
5. Ma P, Yao T, Liu W, Pan Z, Chen Y, Yang H, et al. A 7-kW narrow-linewidth fiber amplifier assisted by optimizing the refractive index of the large-mode-area active fiber. High Power Laser Sci Eng. 2024;12:e45. doi:10.1017/hpl.2024.41.
6. Peng L, Liang Y, He X. Transfers to Earth-Moon triangular libration points by Sun-perturbed dynamics. Adv Space Res. 2025;75(3):2837–55.
7. Ablowitz MJ, Ramani A, Segur H. Nonlinear evolution equations and ordinary differential equations of Painleve'type. Lett Nuovo Cim. 1978;23(9):333–8.
8. Chousurin R, Mouktonglang T, Wongsaijai B, Poochinapan K. Performance of compact and non-compact structure preserving algorithms to traveling wave solutions modeled by the Kawahara equation. Numer Algorithms. 2020;85(5):523–41. doi:10.1007/s11075-019-00825-4.
9. Marinov TT, Marinova RS. Solitary wave solutions with non-monotone shapes for the modified Kawahara equation. J Comput Appl Math. 2018;340:561–70.
10. Wazwaz AM. New solitary wave solutions to the modified Kawahara equation. Phys Lett A. 2007;360(4–5):588–92. doi:10.1016/j.physleta.2006.08.068.
11. Yang ZJ, Zhang SM, Li XL, Pang ZG, Bu HX. High-order revivable complex-valued hyperbolic-sine-Gaussian solitons and breathers in nonlinear media with a spatial nonlocality. Nonlinear Dyn. 2018;94:2563–73.
12. Shen S, Yang Z, Li X, Zhang S. Periodic propagation of complex-valued hyperbolic-cosine-Gaussian solitons and breathers with complicated light field structure in strongly nonlocal nonlinear media. Commun Nonlinear Sci Numer Simul. 2021;103:106005. doi:10.1016/j.cnsns.2021.106005.
13. Rajan MSM. Boomerons in a three-coupled NLS system with inhomogeneous dispersion and nonlinearity. Waves Random Complex Media. 2024;34(5):4784–98. doi:10.1080/17455030.2021.1999533.
14. Rajan MSM. Transition from bird to butterfly shaped nonautonomous soliton and soliton switching in erbium doped resonant fiber. Phys Scr. 2020;95(10):105203. doi:10.1088/1402-4896/abb2df.
15. Foroutan M, Manafian J, Ranjbaran A. Optical solitons in (n+1)-dimensions under anti-cubic law of nonlinearity by analytical methods. Opt Quant Electron. 2018;50:97.
16. Qawaqneh H, Manafian J, Alsubaie AS, Ahmad H. Investigation of exact solitons to the quartic Rosenau-Kawahara-Regularized-Long-Wave fluid model with fractional derivative and qualitative analysis. Phys Scr. 2025;100(1):015270. doi:10.1088/1402-4896/ad9d92.
17. Chakrabarty AK, Roshid MM, Rahaman MM, Abdeljawad T, Osman MS. Dynamical analysis of optical soliton solutions for CGL equation with Kerr law nonlinearity in classical, truncated α-fractional derivative, beta fractional derivative, and conformable fractional derivative types. Results Phys. 2024;60(5):107636. doi:10.1016/j.rinp.2024.107636.
18. Raza MZ, Iqbal MAB, Khan A, Almutairi DK, Abdeljawad T. Soliton solutions of the $(2+1)$-dimensional Jaulent-Miodek evolution equation via effective analytical techniques. Sci Rep. 2025;15(1):3495. doi:10.1038/s41598-025-87785-z.
19. Nee J, Duan J. Limit set of trajectories of the coupled viscous Burgers' equations. Appl Math Lett. 1998;11(1):57–61.
20. Shahen NHM, Foyjonnesa, Bashar MH, Tahseen T, Hossain S, Fellah ZEA. Solitary and rogue wave solutions to the conformable time fractional modified kawahara equation in mathematical physics. Adv Math Phys. 2021;2021(3):6668092. doi:10.1155/2021/6668092.
21. Nasreen N, Seadawy AR, Lu D. Construction of soliton solutions for modified Kawahara equation arising in shallow water waves using novel techniques. Int J Mod Phys B. 2020;34(7):2050045. doi:10.1142/s0217979220500459.

22. Bashar MH, Tahseen T, Shahen NH. Application of the Advanced exp $(-\varphi(\xi))$-expansion method to the nonlinear conformable time-fractional partial differential equations. Turkish J Math Comput Sci. 2021;13(1):68–80. doi:10.14419/ijpr.v7i2.19984.
23. Khater MM. De Broglie waves and nuclear element interaction; abundant waves structures of the nonlinear fractional phi-four equation. Chaos Soliton Fract. 2022;163(5):112549. doi:10.1016/j.chaos.2022.112549.
24. Khater M. Analytical and numerical-simulation studies on a combined mKdV-KdV system in the plasma and solid physics. Eur Phys J Plus. 2022;137(9):1–9. doi:10.1140/epjp/s13360-022-03285-3.
25. Khater MM. Nonlinear biological population model; computational and numerical investigations. Chaos Soliton Fract. 2022;162:112388.
26. Helal MA. Soliton solution of some nonlinear partial differential equations and its applications in fluid mechanics. Chaos Soliton Fract. 2002;13(9):1917–29. doi:10.1016/s0960-0779(01)00189-8.
27. Baleanu D, İnç M, Yusuf A, Aliyu AI. Lie symmetry analysis and conservation laws for the time fractional simplified modified Kawahara equation. Open Phys. 2018;16(1):302–10. doi:10.1515/phys-2018-0042.
28. Zayed EME, Gepreel KA. The (G′/G)-expansion method for finding traveling wave solutions of nonlinear partial differential equations in mathematical physics. J Math Phys. 2009;50(1):013502. doi:10.1063/1.3033750.
29. Elgarayhi A, Karawia AA. New double periodic and solitary wave solutions to the modified Kawahara equation. Int J Nonlinear Sci. 2009;7(4):414–9.
30. Ismaeel SM, Wazwaz AM, Tag-Eldin E, El-Tantawy SA. Simulation studies on the dissipative modified Kawahara solitons in a complex plasma. Symmetry. 2022;15(1):57.
31. Yusufoğlu E, Bekir A, Alp M. Periodic and solitary wave solutions of Kawahara and modified Kawahara equations by using Sine-Cosine method. Chaos Soliton Fract. 2008;37(4):1193–7. doi:10.1016/j.chaos.2006.10.012.
32. Mahmood BA, Yousif MA. A novel analytical solution for the modified Kawahara equation using the residual power series method. Nonlinear Dyn. 2017;89:1233–8.
33. Ak T, Karakoc SBG. A numerical technique based on collocation method for solving modified Kawahara equation. J Ocean Eng Sci. 2018;3(1):67–75.
34. Zhang D. Doubly periodic solutions of the modified Kawahara equation. Chaos Soliton Fract. 2005;25(5):1155–60.
35. Biswas A. Solitary wave solution for the generalized Kawahara equation. Appl Math Lett. 2009;22(2):208–10. doi:10.1016/j.aml.2008.03.011.
36. Başhan A. Bell-shaped soliton solutions and travelling wave solutions of the fifth-order nonlinear modified Kawahara equation. Int J Nonlinear Sci Numer Simul. 2021;22(6):781–95. doi:10.1515/ijnsns-2019-0071.
37. Benjamin TB, Bona JL, Mahony JJ. Model equations for long waves in nonlinear dispersive. Philosophic Transacti Royal Society London. Series A. Mathematic Physic Sci. 1972;272(1220):47–78.
38. Abbasbandy S, Shirzadi A. The first integral method for modified Benjamin-Bona–Mahony equation. Commun Nonlinear Sci Numer Simul. 2010;15(7):1759–64.
39. Niu F, Qi J, Zhou Z. Some methods about finding the exact solutions of nonlinear modified BBM equation. Math Problems Eng. 2021;2021(4):1–12. doi:10.1155/2021/5564162.
40. Khan K, Akbar MA. Application of exp-expansion method to find the exact solutions of modified Benjamin-Bona-Mahony equation. World Appl Sci J. 2013;24(10):1373–7.
41. Khan K, Akbar MA, Alam MN. Traveling wave solutions of the nonlinear Drinfel'd-Sokolov-Wilson equation and modified Benjamin-Bona–Mahony equations. J Egypt Math Soc. 2013;21(3):233–40. doi:10.1016/j.joems.2013.04.010.
42. Rady AA, Osman ES, Khalfallah M. The homogeneous balance method and its application to the Benjamin-Bona–Mahoney (BBM) equation. Appl Math Comput. 2010;217(4):1385–90. doi:10.1016/j.amc.2009.05.027.

43. Tang Y, Xu W, Gao L, Shen J. An algebraic method with computerized symbolic computation for the one-dimensional generalized BBM equation of any order. Chaos Soliton Fract. 2007;32(5):1846–52. doi:10.1016/j.chaos.2005.12.022.
44. Chen Y, Li B, Zhang H. Exact solutions for two nonlinear wave equations with nonlinear terms of any order. Commun Nonlinear Sci Numer Simul. 2005;10(2):133–8. doi:10.1016/s1007-5704(03)00121-7.
45. An JY, Zhang WG. Exact periodic solutions to generalized BBM equation and relevant conclusions. Math Appl Sin. 2006;22(3):509–16.
46. Estévez PG, Kuru ŞENGÜL, Negro J, Nieto LM. Travelling wave solutions of the generalized Benjamin-Bona–Mahony equation. Chaos Soliton Fract. 2009;40(4):2031–40.
47. Tzvetkov N. Long time bounds for the periodic KP-II equation. Int Math Res Notices. 2004;2004(46):24 85–96.
48. Salas AH, Frias BA. New periodic and soliton solutions for the Generalized BBM and Burgers-BBM equations. Appl Math Comput. 2010;217(4):1430–4. doi:10.1016/j.amc.2009.05.068.
49. Gómez CA, Salas AH. Exact solutions for the generalized BBM equation with variable coefficients. Math Probl Eng. 2010;2010:498249.
50. Asjad MI, Munawar N, Muhammad T, Hamoud AA, Emadifar H, Hamasalh FK, et al. Traveling wave solutions to the Boussinesq equation via Sardar sub-equation technique. AIMS Math. 2022;7(6):11134–49. doi:10.3934/math.2022623.
51. Mohammed PO, Agarwal RP, Brevik I, Abdelwahed M, Kashuri A, Yousif MA. On multiple-type wave solutions for the nonlinear coupled time-fractional schrödinger model. Symmetry. 2024;16(5):553.
52. Rehman HU, Iqbal I, Subhi Aiadi S, Mlaiki N, Saleem MS. Soliton solutions of Klein-Fock–Gordon equation using sardar subequation method. Mathematics. 2022;10(18):3377. doi:10.3390/math10183377.
53. Yasin S, Khan A, Ahmad S, Osman MS. New exact solutions of (3+1)-dimensional modified KdV-Zakharov-Kuznetsov equation by Sardar-subequation method. Opt Quant Electron. 2024;56(1):90. doi:10.1007/s11082-023-05558-2.